Spectrochimica Acta Part A 76 (2010) 130–136

Contents lists available at ScienceDirect

Spectrochimica Acta Part A: Molecular and Biomolecular Spectroscopy

journal homepage: www.elsevier.com/locate/saa

Structural conformations and vibrational spectral study of chloroflavone with density functional theoretical simulations

Y. Erdogdu[a,*], O. Unsalan[b], D. Sajan[c], M.T. Gulluoglu[a]

[a] Department of Physics, Ahi Evran University, 40040, Kirsehir, Turkey
[b] Department of Physics, Istanbul University, 34459, Istanbul, Turkey
[c] Department of Physics, Bishop Moore College, Mavelikara, Alappuzha 690110, Kerala, India

ARTICLE INFO

Article history:
Received 25 November 2009
Received in revised form 22 February 2010
Accepted 26 February 2010

Keywords:
Infrared spectra
Raman Spectra
Density functional theory
6-Chloroflavone

ABSTRACT

NIR-FT Raman and FT-IR spectra of 6-chloroflavone were recorded and analyzed. The vibrational wavenumber of the compound have been computed using B3LYP/6-31++G(d,p) level to derive the equilibrium geometry, conformational stability, molecular orbital energies and vibrational wavenumbers. The carbonyl stretching vibrations have been lowered due to conjugation and hydrogen bonding in the molecules. The assignment of fundamental vibrations agrees well with the calculated wavenumbers.

1. Introduction

Flavonoids are a large group of plant secondary metabolites that share a basic phenylbenzopyrone feature and are found in all vascular plants where they occur in several structurally and biosynthetically related classes [1]. They are important constituents of the human diet [2] and can also be found expressive amounts in many medicinal plants [3]. Flavonoid is any member of a class of widely distributed biological natural products containing aromatic heterocyclic skeleton of flavan (2-phenylbenzopyran) but no nitrogen in plants. Generally, flavonoids are biological pigments providing colors from red to blue in flowers, fruit and leaves. Besides their coloring in plants, flavonoids have important roles in the growth and development of plants: protection against UV-B radiation, forming antifungal barriers; antimicrobial, insecticidal and oestrogenic activities; and plant reproduction [4]. Flavonoids have been investigated by X-ray crystallography [5], electron spin resonance [6], FT-IR and Raman spectra [7,11]. Quantum chemical studies of flavonoids at semi-empirical level as well as *ab initio* calculation at the Hartree–Fock level [12–16] have been reported.

The vibrational spectral features of 6-chloroflavone (6C*l*F) molecule have not been subject of detailed analysis so far. NIR-FT Raman spectroscopy combined with quantum chemical computations have recently been used as effective tools in the vibrational analysis of drug molecules, biological compounds and natural product compounds [7,11] since fluorescence free Raman spectra and computed results can help unambiguous identification of vibrational modes as well as the bonding and structural features of complex organic molecular systems. The present work describes the vibrational spectral investigations of 6C*l*F aided by density functional computations to elucidate the correlation between the molecular structure, bonding features and to identify the various modes with greater wavenumber accuracy. Furthermore, we interpreted the calculated spectra in terms of potential energy distributions (TED's) and made the assignment of the experimental bands based on TED analysis results.

2. Experimental

The 6C*l*F sample was purchased from Sigma–Aldrich Chemical Company with a stated purity greater than 98% and it was used as such without further purification. The sample of 6C*l*F is in powder form at room temperature. The infrared spectrum of the sample was recorded between 4000 and 400 cm^{-1} on a Mattson 1000 FTIR spectrometer which was calibrated using polystyrene bands. The sample was prepared as a KBr disc. The FT-Raman spectrum of the sample was recorded between 3500 and 5 cm^{-1} regions on a Bruker FRA 106/S FT-Raman instrument using 1064 nm excitation using Nd:YAG laser. The detector is a liquid nitrogen cooled Ge detector.

3. Computational details

Gaussian 03W and Gauss-view molecular visualization [17–18] software package was used for all theoretical calculations. At first, the structure of the 6C*l*F molecule (Fig. 1) were optimized,

---

[*] Corresponding author. Tel.: +90 0 386 211 46 12; fax: +90 0386 211 45 00.
E-mail address: yusuferdogdu@gmail.com (Y. Erdogdu).

1386-1425/$ – see front matter © 2010 Elsevier B.V. All rights reserved.
doi:10.1016/j.saa.2010.02.043

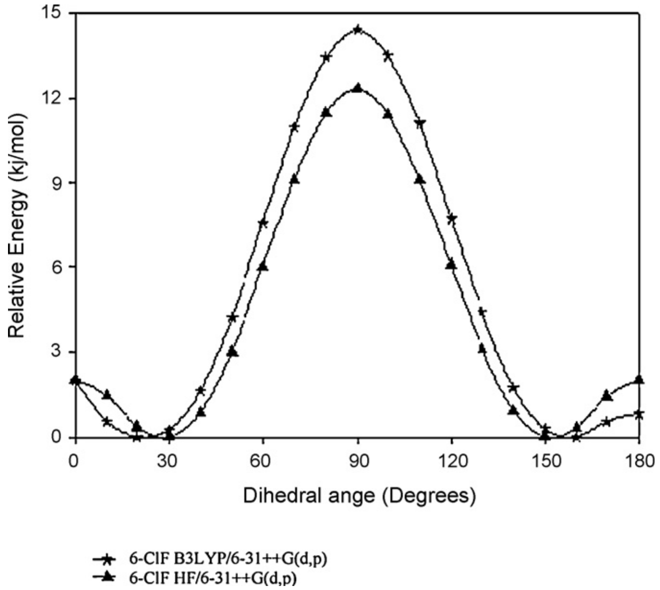

Fig. 1. Torsional barriers for 6-Chloroflavone).

conformational analysis and then the vibrational wavenumbers were calculated with the B3LYP/6-31++G(d,p) basis sets. Harmonic vibrational wavenumbers were calculated using analytic second derivatives to confirm the convergence to minima on the potential surface and to evaluate the zero-point vibrational energies. At the optimized structure of the examined species, no imaginary frequency modes were obtained, proving that a true minimum on the potential energy surface was found. The optimum geometry was determined by minimizing the energy with respected to all geometrical parameters, without imposing molecular symmetry constraints. The theoretical spectrum of 6C*l*F was scaled with 0.967 (for wavenumbers under 1800 cm^{-1}) and 0.955 (for those over 1800 cm^{-1}). The total energy distribution (TED) of vibrational modes was calculated by using the scaled quantum mechanics (SQM) program.

The Raman activities (S_i) calculated with Gaussian 03 program converted to relative Raman intensities (I_i) using the following relationship derived from the intensity theory of Raman scattering.

$$I_i = \frac{f(\upsilon_0 - \upsilon_i)^4 S_i}{\upsilon_i[1 - \exp(hc\upsilon_i/kT)]} \qquad (1)$$

Where υ_0 is the exciting frequency in cm^{-1}, υ_i the vibrational wavenumber of the ith normal mode, h, c and k fundamental constants, and f is a suitably chosen common normalization factor for all peak intensities [19].

4. Results and discussion

4.1. Conformational analysis

The aim of the conformational analysis of the 6C*l*F molecule is to provide a model for the molecular structure. For this reason, the energy barrier of rotation around the C_4–C_{14} bond was calculated for the B3LYP and HF with 6-31++G(d,p) basis sets. The dihedral angle O_{25}–C_4–C_{14}–C_{15} (around C_4–C_{14} bond) was varied form 0° to 180° by steps of 10°. Then, the optimized molecular structure and vibrational normal modes were calculated for ground state in the B3LYP with 6-31++G(d,p) basis sets.

Fig. 1 shows the variation of rotational barriers with the dihedral angles. The calculated relative energies for torsional angle are given in Table 1. The molecular geometry is defined through two effects acting oppositely: a repulsion of the hydrogen atoms in ortho positions on the ring B, which would lead to a staggered conformation of the molecule, and a conjugation effect, which tends to bring phenyl ring in the chromone plane. The equilibrium geometry of the molecule results from a balance between these two effects.

The variation of rotational barriers shows a double-well potential when the dihedral angle varies form 0° to 180°. The two minima occurring at variation of the torsional angles are identical. For this reason, it was satisfactory to optimize only one of the two equivalent minima. These minima are determined α and $180 - \alpha$, the first and second equivalent minima, respectively. Where α is designated O_{25}–C_4–C_{14}–C_{15} dihedral angles.

A maximum is found for a dihedral angle of 90° (E_{90}, perpendicular conformation) with a barrier height of about at 2.953 kcal/mol (HF/6-31++G(d,p)) and 6.274 kcal/mol (B3LYP/6-31++G(d,p)). Nevertheless, other maximum is found for a dihedral angle of 0° (E_0, coplanar conformation). The calculated results show that E_0 has energy ≈2 kcal/mol lower than the E_{90}.

4.2. Molecular orbital energies

The highest occupied molecular orbital (HOMO) energy, the lowest unoccupied molecular orbital (LUMO) energy, and the energy gap between HOMO and LUMO for 6-chloroflavone molecule calculated at the B3LYP/6-31++G(d,p) level of theory and are shown in Table 2. The computed HOMO energies at various conformations of 6-chloroflavone molecule were at −8.048 eV (twisted conformer), −8.103 eV (coplanar conformer) and −7.994 eV (perpendicular conformer). The LUMO energies of 6-chloroflavone molecule were computed at −5.492 eV (twisted conformer), −5.465 eV (coplanar conformer) and −5.220 eV (perpendicular conformer). When the O_{24}–C_4–C_{13}–C_{14} dihedral angle increased, it was seen that the HOMO energies of 6C*l*F increased, while the LUMO energies of 6C*l*F decreased. $\Delta E_{\text{HOMO} - \text{LUMO}}$ energy of were calculated at −2.556 eV (twisted conformation), −2.638 eV (coplanar conformation) and −2.774 eV (perpendicular conformation). This shows that, $\Delta E_{\text{HOMO} - \text{LUMO}}$ energy of twisted conformation (ground state, E_{min}) of 6C*l*F was larger than those of other conformations (coplanar and perpendicular conformation).

In Fig. 2, the dependence of the HOMO and LUMO on the molecular conformation is shown. In all the conformation of 6C*l*F molecule, the HOMO is distributed over benzopyrone ring (A, B rings and halogen atoms). The LUMO is located over the rings without halogen atoms for coplanar and twisted conformations, whereas, it is distributed over benzopyrone ring without halogen atoms for perpendicular conformation.

Table 1
Low and high energy barriers of phenyl rotation computed at various levels of theory for 6-chloroflavone.

		Energy (Hartree)		ΔE (kcal/mol)	
		HF 6-31++G(d.p)	B3LYP 6-31++G(d.p)	HF 6-31++G(d.p)	B3LYP 6-31++G(d.p)
Minimum energy conformation		−1182.51913495	−1187.70611328	0.000	0.000
Transition state	High (E_{90})	−1182.514428320	−1187.696113870	2.953	6.274
	Low (E_0)	−1182.518362980	−1187.699323560	0.484	4.260

Table 2
Bond lengths and bond angles for 6-chloroflavone.

B3LYP/6-31++G(d,p)		X-ray [20]	X-ray [21]	B3LYP/6-31++G(d,p)		X-ray [20]	X-ray [21]
Bond lengths (A°)				Bond angles (°)			
C_1–C_2	1.455	1.448	1.454	C_2–C_1–C_6	113.9	114.1	113.3
C_1–C_6	1.483	1.475	1.468	C_2–C_1–O_{26}	123.4	123.5	123.2
C_1–O_{26}	1.233	1.232	1.223	C_6–C_1–O_{26}	122.5	122.3	123.4
C_2–C_4	1.360	1.354	1.345	C_1–C_2–C_4	122.5	122.4	122.6
C_4–C_{14}	1.475	1.475	1.473	C_2–C_4–C_{14}	126.0	125.8	126.2
C_4–O_{25}	1.364	1.367	1.373	C_2–C_4–O_{25}	121.7	122.2	122.1
C_5–C_6	1.400	1.393	1.383	C_{14}–C_4–O_{25}	112.2	111.9	111.7
C_5–C_{12}	1.399	1.395	1.384	C_6–C_5–C_{12}	121.3	121.6	122.4
C_5–O_{25}	1.371	1.374	1.371	C_6–C_5–O_{25}	121.9	122.3	121.7
C_6–C_7	1.404	1.405	1.408	C_{12}–C_5–O_{25}	116.6	115.9	115.9
C_7–C_9	1.385	1.374	1.367	C_1–C_6–C_5	119.5	119.6	121.2
C_9–C_{10}	1.405	1.397	1.365	C_1–C_6–C_7	121.3	121.8	120.9
C_9–Cl_{27}	1.755	–	1.739	C_5–C_6–C_7	119.0	118.5	117.9
C_{10}–C_{12}	1.388	1.379	1.370	C_6–C_7–C_9	119.5	119.9	119.1
C_{14}–C_{15}	1.406	1.400	1.384	C_7–C_9–C_{10}	121.1	119.1	122.0
C_{14}–C_{23}	1.406	1.399	1.382	C_7–C_9–Cl_{27}	119.9	–	119.0
C_{15}–C_{17}	1.394	1.391	1.388	C_{10}–C_9–Cl_{27}	118.9	–	118.9
C_{17}–C_{19}	1.397	1.393	1.375	C_9–C_{10}–C_{12}	119.7	119.5	119.9
C_{19}–C_{21}	1.398	1.380	1.369	C_5–C_{12}–C_{10}	119.1	119.5	118.6
C_{21}–C_{23}	1.393	1.385	1.391	C_4–C_{14}–C_{15}	120.4	120.8	120.8
				C_4–C_{14}–C_{23}	120.6	121.1	120.7
				C_{15}–C_{14}–C_{23}	118.8	119.3	118.5
				C_{14}–C_{15}–C_{17}	120.4	120.0	120.6
				C_{15}–C_{17}–C_{19}	120.2	119.9	120.1
				C_{17}–C_{19}–C_{21}	119.6	119.9	119.9
				C_{19}–C_{21}–C_{23}	120.2	119.4	119.6
				C_{14}–C_{23}–C_{21}	120.4	121.2	121.0
				C_4–O_{25}–C_5	120.1	120.2	120.2

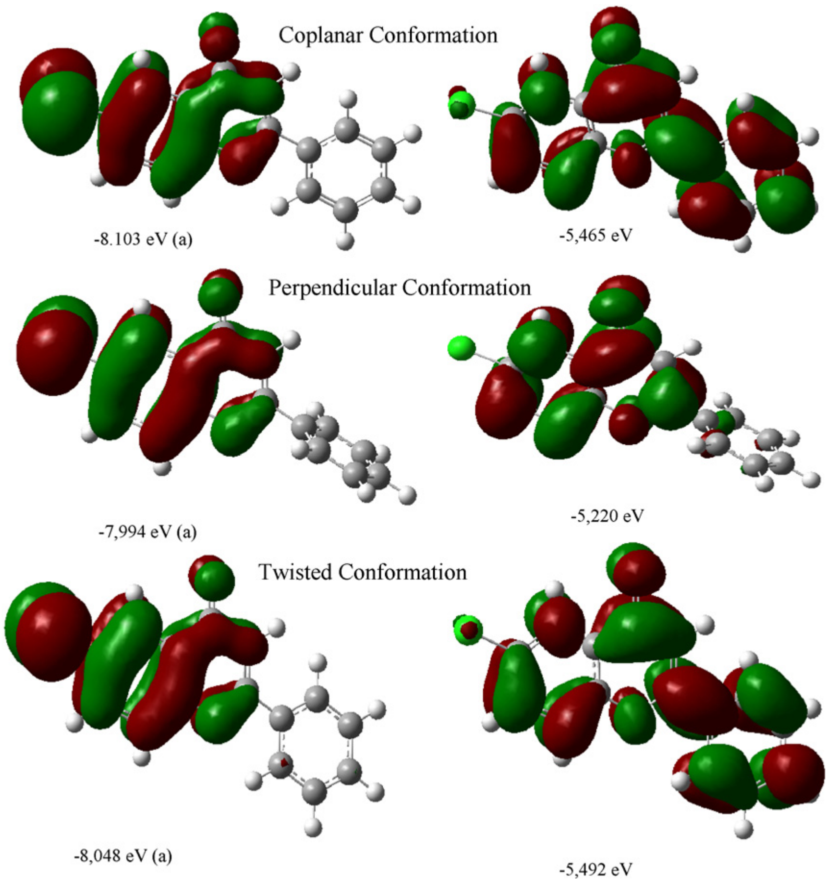

Fig. 2. The HOMO (a) and LUMO (b) plots of all conformation of 6-chloroflavone for B3LYP/6-31++G(d,p).

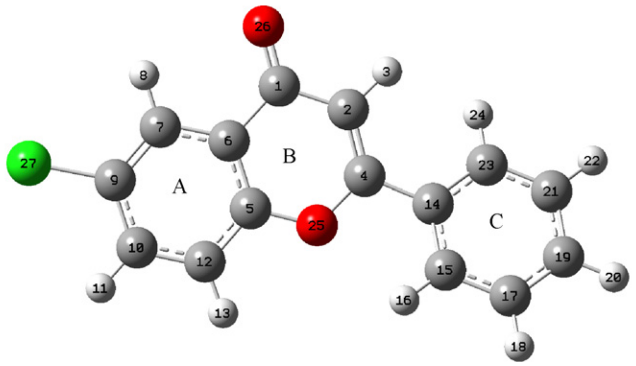

Fig. 3. Molecular structure and atomic numbering of 6-chloroflavone.

4.3. Geometry optimization

The structural parameters of the optimized molecular structure of the 6ClF was calculated with DFT/B3LYP level using 6-31++G(d,p) as basis set. The molecular structure of 6ClF is shown in Fig. 3. Calculated geometric parameters and definitions of the natural co-ordinates for the molecules are summarized in Table 2. The X-ray data of the flavone was reported by Waller et al. [20]. The crystal data of 6ClF are not available in the literature. Therefore, optimized geometric parameters of 6ClF compared with those of flavone [20] and 3,30-[o-phenylenebis(methyleneoxy)]-bis(6-chloroflavone) [21].

The dihedral angle between the phenyl and the pyrone ring is small as expected in the preferred conformation of flavones. The small dihedral angle results in a relatively short C_4–C_{14} bond length are consistent with bond lengths and dihedral angles found in other flavones [22]. When the O_{25}–C_4–C_{13}–C_{14} dihedral angle increased, it was seen that the C_4–C_{13} bond length was also increased.

The O_{25}–C_4–C_{14}–C_{15} dihedral angle and C_4–C_{14} bond distance of the 6ClF are determined at 20.76° and 1.475 (B3LYP/6-31++G(d,p)) A°, respectively. Dihedral angle was determined at 20.82° and C_4–C_{14} bond distance was determined 1.507 A° in the flavone molecule for HF/STO-3G level of theory [23]. Flavone-3′-sulfonamide has a dihedral angle of 8.2° and the C_4–C_{14} bond length of 1.478 (3) A° [24]. In 5-hydroxyflavone, the dihedral angle is 5.2° and the C_4–C_{14} bond length is 1.465 A° [25]. The 5,7-dihydroxy-4′-methoxyflavone with a dihedral angle of 3.1° has a C_4–C_{14} bond length of 1.453 A° [26]. However, in 2′-methyl-3′-nitroflavone, the dihedral angle is 139.8° and the C_4–C_{14} bond length is 1.491 A° [27], and in 5,4′-dihydroxy-3,6,7,8-tetramethoxyflavone a large dihedral angle of 164.4° and a C_4–C_{14} bond length of 1.503 A° were found by Vijayalakshmi et al. [28].

4.4. Vibrational analysis

The vibrational spectral analysis of 6ClF molecule is based on FT-IR (Fig. 4) and Raman (Fig. 5) spectra and scaled vibrational spectrum computed using density functional theory at B3LYP/6-31++G(d,p) level. The 6ClF molecule consists of 27 atoms, which has 75 normal modes. The 75 normal modes of 6ClF have been assigned according to the detailed motion of the individual atoms. This molecule belongs to C_1 symmetry group.

The computed vibrational wavenumbers and the atomic displacements corresponding to the different normal modes are used for identifying the vibrational modes unambiguously. The calculated vibrational wavenumbers, measured infrared and Raman band positions and their assignments are given in Table 3. Total energy distribution (TED) was calculated by using the scaled quantum mechanic program (SQM) and fundamental vibrational modes were characterized by their TED.

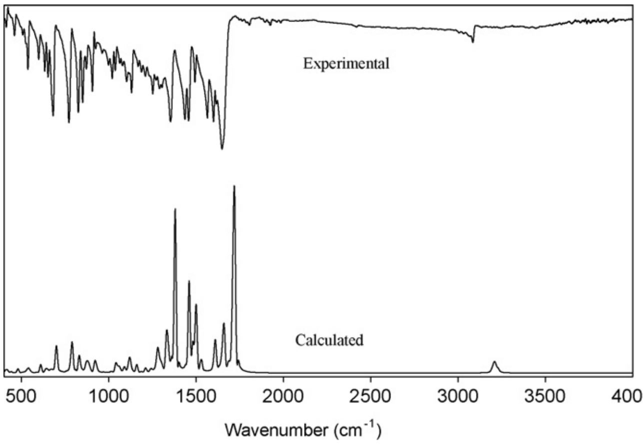

Fig. 4. The infrared spectra of 6-chloroflavone.

The aromatic carbon-hydrogen stretching vibrations appear in the region 3100–3000 cm^{-1}, in-plane C–H bending vibrations in the range of 1000–1300 cm^{-1} and out-of-plane C–H bending vibrations in the range of 750–1000 cm^{-1} [12,29]. For 6ClF, the C–H stretching vibrations predicted at 3097–3042 cm^{-1} for B3LYP/6-31++G(d,p) level of theory. These vibrations observed experimentally at 3033, 3066 and 3086 cm^{-1} in the FT-IR spectrum for 6ClF and the corresponding Raman bands are observed at 3048 and 3073 cm^{-1}. In flavone, IR spectrum bands at 3040, 3059, 3070 and 3100 cm^{-1} corresponds to the C–H stretching vibrations [7,11]. A comparison with the results from the normal mode analysis of 6C/F shows that the aromatic C–H stretching vibrations around 3070 cm^{-1} remain altered by chlorine substitution.

In-plane C–H bending vibrations are observed in the range of 1064–1273 cm^{-1} for 6ClF in the FT-IR spectra. The in-plane bending vibration of chromone part in 6ClF is observed as intense band at 1211 cm^{-1} in IR and the corresponding calculated value is 1223 cm^{-1}. In-plane C–H bending vibrations of 6ClF molecule observed at 1064, 1080, 1168, 1253 and 1273 cm^{-1} in the FT-IR spectra which is mixed with υ_{CC} vibrations. In-plane C–H bending vibrations of 6ClF is well supported with those of the flavone molecules [7,11]. The out-of-plane C–H bending vibrations of 6ClF is observed at 873 and 878 cm^{-1} in IR and Raman spectra respectively, is well supported by the computed values. The band corresponding to C–H in-plane mode of benzene are found at 1292 and 1168 cm^{-1} in the infrared spectrum, corresponding Raman bands are identi-

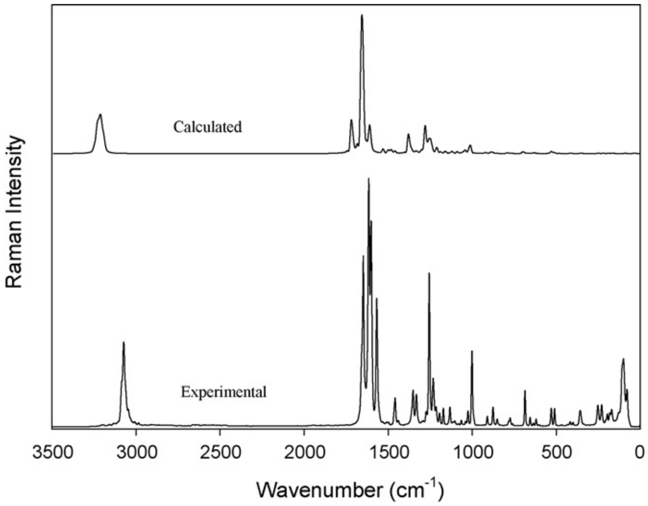

Fig. 5. Raman spectra of the 6-chloroflavone.

Table 3

Comparison of the observed and calculated vibrational spectra of free 6-chloroflavone.

	B3LYP/6-31++G(d.p)				Exp. IR.		Exp. RA		TED (%)[e]
	Freq.[a]	Freq.[b]	I_{IR}[c]	I_{RA}[d]	6C*l*F	Flv	6C*l*F	Flv	
ν_1	33	32	0.077	2.724		–			$\Gamma_{\mathrm{CCCO}}(39)$ $\Gamma_{\mathrm{COCC}}(14)$ R $\Gamma_{\mathrm{CCCC}}(23)$ P
ν_2	41	40	0.009	0.510		–			$\Gamma_{\mathrm{CCCC}}(44)$ $\Gamma_{\mathrm{CCCO}}(13)$ P
ν_3	88	85	0.016	0.588		–	78 vw		$\delta_{\mathrm{CCC}}(35)$ $\Gamma_{\mathrm{CCCC}}(11)$ P $\delta_{\mathrm{CCO}}(18)$
ν_4	105	101	0.079	0.134		–	99 m	94 m	$\Gamma_{\mathrm{CCCC}}(27)$ $\Gamma_{\mathrm{CCCO}}(23)$
ν_5	153	148	0.064	0.168		–		123 w	$\Gamma_{\mathrm{CCCC}}(38)$ $\Gamma_{\mathrm{CCCO}}(22)$
ν_6	167	162	0.745	0.252		–	168 vw	144 w	$\Gamma_{\mathrm{COCC}}(18)$ $\Gamma_{\mathrm{ClCCC}}(15)$
ν_7	188	182	0.185	0.230		–	180 vw	215 m	$\delta_{\mathrm{ClCC}}(37)$ $\delta_{\mathrm{CCC}}(14)$
ν_8	220	213	0.133	0.321		–	229 w		$\Gamma_{\mathrm{CCCC}}(22)$ P
ν_9	248	240	0.254	0.303		–	252 w	267 w	$\delta_{\mathrm{CCC}}(19)$ P $\upsilon_{\mathrm{CC}}(13)$ P-R
ν_{10}	330	319	0.318	0.023		–		294 w	$\delta_{\mathrm{CCC}}(28)$ P $\upsilon_{\mathrm{CC}}(13)$ $\delta_{\mathrm{CCO}}(13)$ R
ν_{11}	349	337	0.484	0.161		–			$\delta_{\mathrm{ClCC}}(37)$ $\delta_{\mathrm{CCC}}(19)$ $\delta_{\mathrm{CCO}}(14)$
ν_{12}	362	350	0.223	0.074		–	356 w		$\Gamma_{\mathrm{CCCO}}(18)$ $\Gamma_{\mathrm{ClCCC}}(16)$ $\Gamma_{\mathrm{CCCC}}(12)$ $\Gamma_{\mathrm{ClCCH}}(10)$
ν_{13}	410	397	0.273	1.401			398 vw		$\upsilon_{\mathrm{ClC}}(23)$ $\delta_{\mathrm{CCC}}(18)$
ν_{14}	416	402	1.723	7.799	415 vw	–	414 vw		$\Gamma_{\mathrm{CCCC}}(64)$ $\Gamma_{\mathrm{CCCH}}(33)$ P
ν_{15}	441	426	0.355	0.443			429 vw		$\Gamma_{\mathrm{CCCC}}(42)$ $\Gamma_{\mathrm{CCCH}}(13)$
ν_{16}	479	463	1.355	1.399	460 w	457 vw	465 vw	454 vw	$\Gamma_{\mathrm{CCCC}}(32)$ $\Gamma_{\mathrm{CCCH}}(20)$ P
ν_{17}	515	498	0.336	20.53	508 vw	509	510 w	510 m	$\delta_{\mathrm{CCC}}(26)$ $\delta_{\mathrm{CCO}}(21)$ $\delta_{\mathrm{COC}}(17)$
ν_{18}	531	513	0.796	21.31		–			$\delta_{\mathrm{CCC}}(28)$ $\upsilon_{\mathrm{CC}}(20)$ $\delta_{\mathrm{CCO}}(16)$
ν_{19}	544	526	2.189	0.343	537 m	529 w	529 w	527 w	$\Gamma_{\mathrm{CCCH}}(34)$ $\Gamma_{\mathrm{CCCC}}(33)$
ν_{20}	610	590	2.739	0.809	599 m	606 m	598 vw		$\delta_{\mathrm{CCO}}(39)$ $\delta_{\mathrm{CCC}}(22)$
ν_{21}	631	610	0.031	6.148		–	618 vw	616 w	$\Gamma_{\mathrm{CCCC}}(59)$ $\Gamma_{\mathrm{CCCH}}(21)$ P
ν_{22}	644	623	2.194	2.018	634 m		636 vw		$\delta_{\mathrm{CCC}}(26)$ $\upsilon_{\mathrm{CCl}}(14)$
ν_{23}	666	644	1.242	2.227	653 m	650 w	655 vw	649 vw	$\Gamma_{\mathrm{CCCC}}(30)$ $\Gamma_{\mathrm{CCCO}}(12)$ P
ν_{24}	684	661	0.263	1.921		673 m		674 m	δ_{CCC} (29) $\upsilon_{\mathrm{CC}}(11)$ $\upsilon_{\mathrm{CCl}}(10)$
ν_{25}	696	673	4.274	15.29	682 s	687 m	686 m		$\Gamma_{\mathrm{CCCC}}(33)$ $\Gamma_{\mathrm{CCCO}}(11)$ $\Gamma_{\mathrm{CCCH}}(10)$
ν_{26}	702	679	7.663	0.311		756 m		745	$\Gamma_{\mathrm{CCCH}}(49)$ $\Gamma_{\mathrm{CCCC}}(21)$ P
ν_{27}	762	737	0.134	0.659					$\upsilon_{\mathrm{CC}}(33)$ R $\upsilon_{\mathrm{CC}}(10)$ P
ν_{28}	786	760	8.530	2.728		–			$\Gamma_{\mathrm{CCCH}}(24)$ $\Gamma_{\mathrm{CCCO}}(19)$ $\Gamma_{\mathrm{CCCC}}(16)$
ν_{29}	792	766	5.774	1.977	772 s	769 s	774 vw	768	$\Gamma_{\mathrm{CCCH}}(55)$ $\Gamma_{\mathrm{CCCC}}(11)$ P
ν_{30}	833	805	7.382	0.084					$\Gamma_{\mathrm{CCCH}}(47)$ $\Gamma_{\mathrm{OCCH}}(24)$ $\Gamma_{\mathrm{ClCCH}}(13)$
ν_{31}	856	828	0.600	1.398	826 s				$\Gamma_{\mathrm{CCCH}}(22)$ $\Gamma_{\mathrm{OCCH}}(19)$ P
ν_{32}	874	845	5.111	1.472	850 m	851 m	852 vw	850 vw	$\Gamma_{\mathrm{CCCH}}(56)$ P $\delta_{\mathrm{CCC}}(10)$ R
ν_{33}	885	856	3.543	8.755	873 w	868 w	877 w	904 w	$\delta_{\mathrm{CCH}}(18)$ $\Gamma_{\mathrm{CCCC}}(14)$ $\delta_{\mathrm{CCC}}(10)$ P
ν_{34}	921	891	3.712	3.416					$\delta_{\mathrm{OCC}}(16)\delta_{\mathrm{COC}}(13)$ $\delta_{\mathrm{CCC}}(11)$
ν_{35}	929	899	1.700	0.040	906 m	906 m	909 vw		$\Gamma_{\mathrm{CCCH}}(58)$ $\Gamma_{\mathrm{ClCCH}}(25)$
ν_{36}	943	912	0.243	0.146	927 vw	925 vw			Γ_{CCCH} (54) $\Gamma_{\mathrm{HCCH}}(26)$ P
ν_{37}	969	937	0.190	0.043		–			υ_{CC} (45) $\delta_{\mathrm{CCC}}(35)$ P
ν_{38}	989	957	0.098	0.316	963 vw	–			$\Gamma_{\mathrm{CCCH}}(26)$ $\Gamma_{\mathrm{HCCH}}(38)$ $\Gamma_{\mathrm{HCCCl}}(12)$
ν_{39}	1009	976	0.007	0.604		–			$\Gamma_{\mathrm{HCCH}}(50)$ $\Gamma_{\mathrm{HCCC}}(32)$ P
ν_{40}	1014	980	0.388	30.13	1000 vw	1011 w	1002 m	1000 s	$\upsilon_{\mathrm{CC}}(35)$ $\upsilon_{\mathrm{CO}}(11)$ R $\delta_{\mathrm{CCC}}(17)$ $\delta_{\mathrm{CCH}}(18)$ P
ν_{41}	1044	1009	5.304	10.61	1020 w	1029 m	1023 w	1012 m	$\Gamma_{\mathrm{HCCH}}(68)$ $\Gamma_{\mathrm{CCCH}}(15)$ P
ν_{42}	1062	1027	2.124	1.474	1038 w	1044 m	1039 vw	1044 vw	$\upsilon_{\mathrm{CC}}(25)$ P $\upsilon_{\mathrm{CC}}(18)$ R
ν_{43}	1088	1052	2.066	3.891	1064 vw				$\upsilon_{\mathrm{CC}}(32)$ R $\delta_{\mathrm{CCH}}(27)$ $\upsilon_{\mathrm{CC}}(14)$ P
ν_{44}	1111	1074	1.871	0.562	1080 vw	1079 w			$\upsilon_{\mathrm{CC}}(47)$ $\delta_{\mathrm{CCH}}(20)$ P
ν_{45}	1123	1086	6.262	4.545	1103 w	1101 m	1100 m	1100 vw	$\upsilon_{\mathrm{CC}}(44)$ $\upsilon_{\mathrm{CCl}}(10)$ R
ν_{46}	1160	1122	2.640	3.576	1131 m	1129 s	1131 vw	1131 vw	$\upsilon_{\mathrm{CC}}(59)$ $\delta_{\mathrm{CCH}}(17)$ P
ν_{47}	1188	1149	0.094	2.116	1168 vw		1172 vw	1160 vw	$\delta_{\mathrm{CCH}}(25)$ R $\upsilon_{\mathrm{CC}}(26)$ P
ν_{48}	1211	1171	1.596	9.159	1189 vw	–	1193 vw	1191 w	$\upsilon_{\mathrm{CC}}(48)$ $\delta_{\mathrm{CCH}}(25)$
ν_{49}	1243	1202	1.315	12.24		–			$\delta_{\mathrm{CCH}}(72)$ $\upsilon_{\mathrm{CC}}(18)$ P
ν_{50}	1255	1213	0.385	30.10	1211 vw	1226 m	1214vw	1235 s	$\delta_{\mathrm{CCH}}(60)$ $\upsilon_{\mathrm{CC}}(25)$ P
ν_{51}	1277	1235	9.982	46.75	1253 m	1260 m	1255 s	1266 s	$\delta_{\mathrm{CCH}}(26)$ $\upsilon_{\mathrm{CC}}(18)$ R-P $\upsilon_{\mathrm{CC}}(26)$
ν_{52}	1294	1251	6.334	5.994	1273 vw	1283 w	1274 vw		$\delta_{\mathrm{CCH}}(47)$ $\upsilon_{\mathrm{CC}}(12)$ R-P $\upsilon_{\mathrm{CC}}(10)$
ν_{53}	1334	1290	22.48	3.449	1292 vw	–			$\upsilon_{\mathrm{CC}}(56)$ $\upsilon_{\mathrm{CO}}(25)$ R
ν_{54}	1365	1320	1.202	0.720		1311 w	1332 m	1334 m	$\delta_{\mathrm{CCH}}(60)$
ν_{55}	1366	1321	1.629	10.40				1374 w	$\delta_{\mathrm{CCH}}(70)$P
ν_{56}	1379	1334	56.00	20.19	1354 s	1376 s	1351 m		$\delta_{\mathrm{CCH}}(20)$ $\upsilon_{\mathrm{CO}}(21)$ $\upsilon_{\mathrm{CC}}(16)$
ν_{57}	1459	1411	32.58	2.147	1437 s	1449 m	1438	1449 w	$\upsilon_{\mathrm{CC}}(48)$ $\delta_{\mathrm{CCH}}(10)$
ν_{58}	1484	1435	11.52	4.635					$\delta_{\mathrm{CCH}}(47)$ $\upsilon_{\mathrm{CC}}(24)$ P
ν_{59}	1499	1450	22.57	2.448	1458 s	1466 s	1457 m	1469 w	$\delta_{\mathrm{CCH}}(49)$ $\upsilon_{\mathrm{CC}}(28)$
ν_{60}	1531	1480	3.546	3.347	1494 m	1495 s			$\delta_{\mathrm{CCH}}(59)$ $\upsilon_{\mathrm{CC}}(29)$ P
ν_{61}	1607	1554	14.18	24.10	1565 s	1569 m	1567 s	1571 s	$\upsilon_{\mathrm{CC}}(43)$ R $\upsilon_{\mathrm{CC}}(12)$ P
ν_{62}	1623	1569	0.904	4.297		–			$\upsilon_{\mathrm{CC}}(45)$ $\upsilon_{\mathrm{CC}}(21)$ P
ν_{63}	1646	1592	3.555	14.87	1600 s	1606 m	1602 s	1602 s	$\upsilon_{\mathrm{CC}}(55)$ $\delta_{\mathrm{CCH}}(13)$ P
ν_{64}	1650	1596	0.091	37.15	1618 m		1615 vs		$\upsilon_{\mathrm{CC}}(65)$
ν_{65}	1657	1602	21.03	100					$\upsilon_{\mathrm{CC}}(59)$
ν_{66}	1716	1660	100	30.81	1649 vs	1646 vs	1648 s	1633 vs	$\upsilon_{\mathrm{CO}}(85)$
ν_{67}	3186	3042	0.113	0.534	3033 w	3040 vw	3048 w		$\upsilon_{\mathrm{CH}}(96)$ P
ν_{68}	3195	3051	1.345	1.597		3059 s			$\upsilon_{\mathrm{CH}}(99)$ P
ν_{69}	3205	3061	4.084	1.833	3066 vw	3070 vw		3069 s	$\upsilon_{\mathrm{CH}}(99)$ P
ν_{70}	3212	3067	0.137	0.539		–			$\upsilon_{\mathrm{CH}}(100)$
ν_{71}	3214	3070	2.072	1.671		–			$\upsilon_{\mathrm{CH}}(96)$ P
ν_{72}	3225	3080	0.641	0.692		–			$\upsilon_{\mathrm{CH}}(97)$ P
ν_{73}	3225	3080	0.276	0.383		–			$\upsilon_{\mathrm{CH}}(99)$
ν_{74}	3226	3081	1.270	2.277					$\upsilon_{\mathrm{CH}}(99)$

Table 3 (*Continued*)

	B3LYP/6-31++G(d.p)				Exp. IR.		Exp. RA		TED (%)[e]
	Freq.[a]	Freq.[b]	I_{IR}[c]	I_{RA}[d]	6ClF	Flv	6ClF	Flv	
ν_{75}	3243	3097	0.295	0.947	3086 vs	3100 vw	3073 vs	3135 vw	$\upsilon_{CH}(98)$

P: phenyl (C ring), R: A and B rings, υ: stretching, δ: bending, Γ: torsion, vs, very strong; s, strong; m, medium; w, weak; vw, very weak, Flv: flavone, 6ClF: 6-vhloroflavone.

[a] Unscaled frequencies.

[b] Obtained from the wavenumbers calculated at B3LYP/6-31++G(d,p) using scaling factors 0.967 (for wavenumbers under 1800 cm^{-1}) and 0.955 (for those over 1800 cm^{-1}).

[c] Relative absorption intensities normalized with highest peak absorption equal to 100.

[d] Relative Raman intensities calculated by Eq. (1) and normalized to 100.

[e] Total energy distribution calculated B3LYP/6-31++G(d,p) level of theory. Only contributions ≥10% are listed.

fied at 1172 cm^{-1}. The C–H in-plane mode is found as weak IR band at 1131 cm^{-1} and weak Raman band at 1131 cm^{-1}. The intense IR band at 772 and 682 cm^{-1} and the corresponding Raman band at 774 and 686 cm^{-1} are identified as CH out-plane bend of C-ring. The theoretical wavenumbers of C–H in-plane and out-of-plane is well supported with those of the experimental ones.

The carbonyl bands are most characteristic bands of the IR and Raman spectrum and for this reason; such bands have been the subject of extensive studies [29–30]. The intensity of C=O stretch increases due to conjugation or the formation of hydrogen bonds. The increase in conjugation therefore leads to intensification of Raman lines as well as increased infrared band intensities. In 6ClF the C=O bond is conjugated with the γ-pyrone ring. The carbonyl stretching wavenumber of flavone is observed in the range 1670–1625 cm^{-1}[7–12]. The most intensive peak is the C=O stretching which are observed at 1646 cm^{-1} (IR), 1633 cm^{-1} (RA) for flavones. The very strong intense band at 1649 cm^{-1} in IR and strong intense band at 1648 cm^{-1} in Raman can be assigned to C=O stretch for 6ClF [7–12]. The results of computations give the wavenumber of this mode at 1660 cm^{-1}. The lowering of the C=O stretching wavenumber is due an increase in the π-conjugation between the B ring and pyrone part through the inter-ring bond. The torsion angle between the side phenyl group and the rest of the molecule strongly influence the π-electrons distribution. In solid state, the dihedral angle is smaller due to the constraints induced by effect of intermolecular interaction in the crystal, which results in a stronger π-electron delocalization [30–32]. Hence the lowering of the carbonyl stretching mode can be attributed to the conjugation and intermolecular hydrogen bonding. The C–C=O bending mode of 6ClF is observed in IR spectrum at 599 cm^{-1} and the corresponding Raman band at 598 cm^{-1},which is well supported by B3LYP/6-311++G(d,p) level of theory. The C–C=O bending mode of flavone is observed at 606 cm^{-1} (IR) and 616 cm^{-1} (Raman).

The C=C stretching vibration of the flavone derivatives is expected around 1618 cm^{-1} [7–12]. The intense band in Raman spectrum at 1615 cm^{-1} are predominantly localized on the $C_2{=}C_4$ double bond of the chromone part, which is not shared between the two ring systems. This bond length is clearly shorter than all other C–C bonds and behaves like a real double bond, which is well supported by $C_2{=}C_4$ bond lengths of similar flavone derivatives [29–32]. The C–O–C stretch is observed as strong band in IR at 1354 cm^{-1} and at 1351 cm^{-1} in Raman. The computed value for this mode is 1334 cm^{-1}. The very strong band at about 1253 cm^{-1} in both IR and Raman spectra corresponds to C_4–C_{14} stretching vibrations and its high intensity is due to mechanical coupling with other ring vibrations [33,34]. The wavenumber of the C_4–C_{14} vibration increases for the crystalline state suggests that the molecule must be planar. Indeed, for a planar structure, the delocalization of π-electron throughout the whole molecule, and particularly across the C–C inter-ring bond, is more pronounced than for a twisted molecule; this delocalization affects the bond length of the C_4–C_{14} bond, which must have a more marked double bond character and so a high wavenumber. Another wavenumber modification is observed in the IR spectrum of 6F/C in the solid state for the C–H in-plane mode of ring C which appears at 1211 cm^{-1}. For a planar structure, this in-plane vibrational mode must be affected by steric interaction between ortho hydrogen (H_{16} and H_{24}) of the ring C and H_3 and the pair of non-bonding electrons O_{25}.

The actual band positions of ring stretching vibrations are determined by the form of constituents around the ring [12,29]. The two doubly degenerate ring stretching modes *8a* and *8b* (1600 cm^{-1}) and *19a* and *19b* (1490 cm^{-1}) and the two non-degenerate modes of benzene *14* (1300 cm^{-1} and *1* (998 cm^{-1}), corresponds to C–C skeletal vibrations [35]. The doubly degenerate vibrational modes split up into two distinct wavenumbers because of the lowering of symmetry. The e_{2g} (8a and 8b) vibration consists of dilation and contraction of the ring, produced mainly by stretching and compression of the bonds. The frequency of vibrational pair *8* in monosubstituted benzene is rather insensitive of substitution. The phenyl ring mode 8a manifests as very intense bands in IR and Raman spectra at 1600 and 1602 cm^{-1}respectively [24,34,35]. Its relatively weaker companion 8b is observed in infrared spectra at 1565 cm^{-1} and as intense band in Raman at 1567 cm^{-1}.The frequency of vibration 19 in monosubstituted benzene derivative is insensitive of substitution. This 19a mode can be expected in the range 1470–1515 cm^{-1} with higher intensity and 19b in the range 1440–1470 cm^{-1} as weak band [33,36]. The modes corresponding to 19a is observed at 1494 cm^{-1} in IR spectrum. 19b can be observed as a strong band at 1437 cm^{-1} in IR spectrum and at 1449 cm^{-1} in Raman spectrum.

In benzene, the fundamentals 1 (997 cm^{-1}) and 12 (1010 cm^{-1}) representing the ring-breathing and trigonal bending modes, respectively give rise to combined modes in molecules belonging to reduced symmetry. The strong bands at 1000 cm^{-1} in Raman and medium band at 1012 cm^{-1} in Raman can be identified as 1 and 12 modes of C ring [33,35]. The medium intense band at 634 cm^{-1} in IR and weak band at 636 cm^{-1} in Raman is assigned to 6b mode of benzene [33–36]. The modes corresponding to 16a is observed as weak bands in IR spectrum at 460 cm^{-1}, the corresponding Raman bands is observed at 465 cm^{-1}respectively, which is supported by computations as well.

The C–Cl absorption is observed in the broad region between 850–550 cm^{-1} depending on the configuration and conformation of the compound [37]. When several chlorine atoms are attached to one carbon atom, the band is usually more intense and at high frequency end of the assigned limits. The band at 634 cm^{-1} in IR and 636 cm^{-1} in Raman band attributed to the C–Cl stretching vibration (ν_{22}) which is coupled with 6b mode. The in-plane C–Cl deformation vibrations are obtained at a low frequency region of the Raman spectra corresponding to 398 cm^{-1}. The out-of-plane C–Cl modes are assigned to the Raman wavenumber at 180 cm^{-1}. These assignments are in good agreement with the literature [37]. The asymmetric C–Cl is stretching moderately overlapped with the C–C stretch and C–H in-plane bending modes, whereas the symmetric C–Cl stretching is mixed with the C–C and C–H stretching mode. C–Cl out of plane vibrations effectively mixed with each other and also the in-plane C–H and C–C bending vibrations contributed to C–C*l* deformation.

5. Conclusion

The NIR-FT Raman and FT-IR spectra of 6C*l*F molecule have been recorded and analyzed. Density functional theory (DFT) calculations at the B3LYP/6-31++G(d,p) level has been used to compute energies of different conformers of 6C*l*F to find out their stability, the optimized geometry of the most stable conformer and its vibrational spectrum.

The vibrational modes were assigned on the basis of TED analysis and analyzed by using SQM program. The carbonyl stretching vibrations have been lowered due to conjugation and hydrogen bonding in the molecules. The observed vibrational wavenumbers and optimized geometric parameters were seen to be in good agreement with the experimental data.

Acknowledgement

This work was supported by the Research Fund of Ahi Evran University Project Numbers: A10/2009. We wish to thank the central laboratory of METU for Raman spectral recording and Gazi University Art and Science Faculty Department of Chemistry for infrared spectral recording. We wish thanks to Assoc. Prof. Dr Mustafa KURT for Gaussian 03W program package.

References

[1] J.B. Harborne, C.A. Williams, Phytochemistry 55 (6) (2000) 481–504.
[2] S. Karakaya, N.E.L. Sedef, Food Chem. 66 (3) (1999) 289–292.
[3] E. Middleton, C. Kandaswami, T.C. Theoharides, Pharm. Rev. 52 (4) (2000) 673–751.
[4] http://chemicalland21.com/fc/FLAVONES.htm.
[5] M.C. Etter, Z. Urbanczyk-Lipowska, S. Baer, P.F. Barbara, J. Mol. Struct. 144 (1986) 155–167.
[6] S. van Acker, A.B.E. de Groot, M.J. van den Berg, D.J. Tromp, G. Donne-Op den, M.N.L. Kelder, G. van der Vigh, W.J.F. Bast, Chem. Res. Toxicol. 9 (1996) 1305–1317.
[7] J.P. Cornard, J.C. Merlin, A.C. Boudet, L. Vrielynk, Biospectroscopy 3 (1997) 183–193.
[8] J.P. Abraham, D. Sajan, J. Mathew, I.H. Joe, V. George, V.S. Jayakumar, J. Raman Spectrosc. 39 (2008) 1821–1831.
[9] Y. Erdogdu, O. Unsalan, M.T. Gulluoglu, Turk. J. Phys. 33 (2009) 249–259.
[10] Y. Erdogdu, O. Unsalan, M.T. Gulluoglu, J. Raman Spectrosc., in press.
[11] O. Unsalan, Y. Erdogdu, M.T. Gulluoglu, J. Raman Spectrosc. 40 (5) (2009) 562–570.
[12] L. Vrielynck, J.P. Cornard, J.C. Merlin, M.F. Lautie, Spectrochim. Acta A 50 (1993) 2177–2188.
[13] G.K. Pereira, P.M. Donate, S.E. Galemeck, J. Mol. Struct. (Theochem). 363 (1996) 87–96.
[14] G.K. Pereira, P.M. Donate, S. Galemeck, J. Mol. Struct. (Theochem). 392 (1997) 169–179.
[15] H.M. Ishiki, P.M. Donate, S.E. Galemeck, J. Mol. Struct. (Theochem). 423 (1998) 235–243.
[16] M. Meyer, J. Quantum Chem. 76 (2000) 724–737.
[17] M. J. Frisch, G. W. Trucks, H. B. Schlegel, G. E. Scuseria, M. A. Robb, J. R. Cheeseman, J. A. Montgomery, Jr., T. Vreven, K. N. Kudin, J. C. Burant, J. M. Millam, S. S. Iyengar, J. Tomasi, V. Barone, B. Mennucci, M. Cossi, G. Scalmani, N. Rega, G. A. Petersson, H. Nakatsuji, M. Hada, M. Ehara, K. Toyota, R. Fukuda, J. Hasegawa, M. Ishida, T. Nakajima, Y. Honda, O. Kitao, H. Nakai, M. Klene, X. Li, J. E. Knox, H. P. Hratchian, J. B. Cross, V. Bakken, C. Adamo, J. Jaramillo, R. Gomperts, R. E. Stratmann, O. Yazyev, A. J. Austin, R. Cammi, C. Pomelli, J. W. Ochterski, P. Y. Ayala, K. Morokuma, G. A. Voth, P. Salvador, J. J. Dannenberg, V. G. Zakrzewski, S. Dapprich, A. D. Daniels, M. C. Strain, O. Farkas, D. K. Malick, A. D. Rabuck, K. Raghavachari, J. B. Foresman, J. V. Ortiz, Q. Cui, A. G. Baboul, S. Clifford, J. Cioslowski, B. B. Stefanov, G. Liu, A. Liashenko, P. Piskorz, I. Komaromi, R. L. Martin, D. J. Fox, T. Keith, M. A. Al-Laham, C. Y. Peng, A. Nanayakkara, M. Challacombe, P. M. W. Gill, B. Johnson, W. Chen, M. W. Wong, C. Gonzalez, and J. A. Pople, Gaussian 03, Revision C.02, Gaussian, Inc., Wallingford CT, 2004.
[18] A. Firsch-, A.B. Nielsen-, A.L. Holder, Gaussview Users Manual, Gaussian Inc., Pitsburg, 2000.
[19] R. Wysokinski, K. Hernik, R. Szostak, D. Michalska, Chem. Phys. 333 (2007) 37–48.
[20] M.P. Waller, D.E. Hibbs, J. Overgaard, J.R. Hanrahan, T.W. Hambley, Spectrochim. Acta 59 (2003) 767–768.
[21] S. Thinagar, D. Velmurugan, S.S.S. Raj, H.-K. Fun, S.C. Gupta, H. Merazig, S. Bouacida, Acta Cryst. C 59 (2003) 181–183.
[22] B.J. Hall, J.R. Hanrahan, G.A.R. Johnston, T.W. Hambley, D.E. Hibbs, Acta Cryst. E 57 (2001) 592–593.
[23] A. Mantas, E. Deretey, F.H. Ferretti, M. Estrada, I.G. Csizmadia, J. Mol. Struc. (Theochem). 504 (2000) 77–103.
[24] E. Kendi, S. Özbey, O. Bozdag, R. Ertan, Acta Cryst. C 56 (2000) 457–458.
[25] M. Shoja, Acta Cryst. C 46 (1990) 517–519.
[26] M. Shoja, Acta Cryst. C 48 (1992) 2033–2035.
[27] E. Kendi, S. Özbey, M. Tunçbilek, R. Ertan, Cryst. Res. Technol. 5 (1996) 457–458.
[28] J. Vijayalakshmi, S.S. Rajan, R. Srinivasan, A.G. Ramachandran Nair, Acta Cryst. C 42 (1986) 1752–1753.
[29] L. Vrielynck, J.P. Cornard, J.C. Merlin, M.F. Lautie, Spectrochim. Acta A 50 (1994) 2177–2188.
[30] L. Vrielynck, J.P. Cornard, J.C. Merlin, P. Bopp, J. Mol. Struc. 297 (1993) 227–234.
[31] J.P. Cornard, A.C. Boudet, J.C. Merlin, Spectrochim. Acta A 57 (2001) 591–602.
[32] J.P. Cornard, L. Vrielynck, J.C. Merlin, J.C. Wallet, Spectrochim. Acta A 51 (1995) 913–923.
[33] B. Smith, Infrared Spectral Interpretation. A Systematic Approach, CRC Press, Washington, DC, 1999.
[34] F.R. Dollish, W.G. Fateley, F.F. Bentley, Characteristic Raman Frequencies of Organic Compounds, John Wiley & Sons, New York, 1997.
[35] G. Varsanyi, Vibrational Spectra of Benzene Derivatives, Academic press, New York, 1969.
[36] N.B. Colthup, L.H. Daly, S.E. Wiberley, Introduction to Infrared and Raman Spectroscopy, Academic Press, New York, 1990.
[37] J.R. Durig, M.M. Bergana, H.V. Phan, J. Raman Spectrosc. (22) (1991) 141–154.